surprising to learn that many effective solutions exist and that populations consequently diverge in both phenotype and genotype. However, the situation represented in these experiments is the simplest possible: directional selection acting on beneficial mutations that reduce genome size, leading to strong phenotypic convergence and the eventual fixation of a single genotype. The situation is strikingly similar to the evolution of the virus Qβ *in vitro*, where it evolves strongly reduced genome size and increased replication rate[27]. Nevertheless, we have demonstrated not only that the genetic basis of evolutionary change varies between replicate realizations but also that the evolutionary fate of evolving lineages becomes steadily more closely determined through time and is strongly influenced by key innovations involving irreversible epistatic interactions between loci. Thus, even in this simplest of situations, the outcome of evolution can be any of several genotypes, and it cannot be predicted which will emerge in any particular realization. □

Methods

All experiments were conducted using Tierra v.5.0, and run on computers based on Intel Pentium II and Pentium III running the Microsoft Windows 98 and Windows 2000 operating systems. The end points of the small-population and large-population experiments can be downloaded from McGill University's website (http://www.mcgill.ca/biology/faculty/bell).

Basic experiments and 'go-back' experiments

A single copy of the Tierran founder genotype, 80aaa, was used to seed a series of 109 small-population and 20 large-population replicates conducted with the methodology of Yedid and Bell[21]. Evolution was considered to have ceased when the only replication-competent genotypes being produced were nearly neutral variants and no further change in size or fitness seemed possible. Genotypes from two experiments that resulted in the two major products of evolution (27 density-independent (DI) and 22 DI types) were selected for a series of 'go-back' experiments. We extracted a dominant genotype from points near the end, middle and beginning of each experiment, and inoculated the system with that genotype alone, using the same culture conditions as for the original experiment. Ten replicates were run for each genotype. This protocol was repeated for the 20 large-population experiments, except that the starting carrying capacity was 10,000 size-80 creatures.

Test of fitness effects of *div/ifz–ret* combination

Two genotypes from an experiment that resulted in a size 22 DI end point, one of size 56 lacking the *div/ifz–ret* fingerprint and a second of size 54 containing the fingerprint, were selected to investigate whether or not occurrence of the fingerprint by itself conferred enhanced fitness. Dummy instructions were added to a non-critical section of the genome of the size-54 genotype to slow its rate of replication, resulting in a size-57 genotype equal in fitness to the size-56 type. The two genotypes were competed against one another, saving all progeny genotypes so as to trace unequivocally the lineage of subsequent dominant types; the added instructions provided a marker for identifying progeny of the size-54/57 genotype. One set of experiments was inoculated with a single individual of each type at low density; a second set was inoculated with high and equal numbers of each. In the great majority (>90%) of the tests conducted, dominant genotypes derived from the size-54/57 type ultimately prevailed, even in cases where progeny of the size-56 type initially had a short-term advantage.

Determination of end point by *div/ifz–ret* combination

A size-63 genotype from an experiment that resulted in a size-27 DI end point was modified to contain the *div/ifz–ret* fingerprint, and used to inoculate the system as in the 'go-back' experiments. It was found in all attempts that the resulting end points were smaller than size 27 (mostly of size 22) and retained the *div/ifz–ret* fingerprint. A second set of experiments was conducted in which the same size-63 genotype was modified with only the anterior *div* near the creature's head, to examine whether the presence of this instruction was a necessary preadaptation for genotypes smaller than size 27 to occur. Wherever it was retained, a genotype smaller than size 27 was the eventual end point, although the anterior *div* was lost through mutation roughly half the time, resulting in size-27 types with the posterior *div–ret* combination.

Received 14 June; accepted 9 September 2002; doi:10.1038/nature01151.

1. Gould, S. J. *Wonderful Life: The Burgess Shale and the Nature of History* (W. W. Norton, New York, 1989).
2. Dykhuizen, D. Experimental studies of natural selection in bacteria. *Annu. Rev. Ecol Syst.* **21,** 373–398 (1990).
3. Fisher, R. A. *The Genetical Theory of Natural Selection* (Dover, New York, 1930).
4. Atwood, K. C., Schneider, L. K. & Ryan, F. J. Selective mechanisms in bacteria. *Cold Spring Harb. Symp. Quant. Biol.* **16,** 345–355 (1951).
5. Gerrish, P. J. The rhythm of microbial adaptation. *Nature* **413,** 299–302 (2001).
6. Dykhuizen, D. & Hartl, D. L. Evolution of competitive ability in *Escherichia coli*. *Evolution* **35,** 581–594 (1981).
7. Travisano, M., Mongold, J. A., Bennett, A. F. & Lenski, R. E. Experimental tests of the roles of adaptation, chance, and history in evolution. *Science* **267,** 87–90 (1995).
8. Kramer, F. R., Mills, D. R., Cole, P. E., Nishihara, T. & Spiegelman, S. Evolution in vitro: sequence and phenotype of a mutant RNA resistant to ethidium bromide. *J. Mol. Biol.* **89,** 719–736 (1974).
9. Bull, J. J. *et al.* Exceptional convergent evolution in a virus. *Genetics* **147,** 1497–1507 (1997).
10. Nakatsu, C. H. *et al.* Parallel and divergent genotypic evolution in experimental populations of *Ralstonia* sp. *J. Bacteriol.* **180,** 4325–4331 (1998).
11. Lenski, R. & Travisano, M. Dynamics of adaptation and diversification: a 10,000 generation experiment with bacterial populations. *Proc. Natl Acad. Sci. USA* **91,** 6808–6814 (1994).
12. Korona, R., Nakatsu, C. H., Forney, L. J. & Lenski, R. E. Evidence for multiple adaptive peaks from populations of bacteria evolving in a structured habitat. *Proc. Natl Acad. Sci. USA* **91,** 9037–9041 (1994).
13. Travisano, M. Long-term experimental evolution in *Escherichia coli*. VI. Environmental constraints on adaptation and divergence. *Genetics* **146,** 471–479 (1997).
14. Hartley, B. S. Experimental evolution of ribitol dehydrogenase. *Microorganisms as Model Systems for Studying Evolution* (ed. Mortlock, R. P.) 23–54 (Plenum, New York, 1984).
15. Yin, J. Evolution of bacteriophage T7 in a growing plaque. *J. Bacteriol.* **175,** 1272–1277 (1993).
16. Cohan, F. M. & Hoffmann, A. A. Genetic divergence under uniform selection. II. Different responses to selection for knockdown resistance to ethanol among *Drosophila melanogaster* populations and their replicate lines. *Genetics* **114,** 145–163 (1986).
17. Hoffmann, A. A. & Harshman, L. G. Desiccation and starvation resistance in *Drosophila*: Patterns of variation at the species, population and intrapopulation levels. *Heredity* **83,** 637–643 (1999).
18. Ray, T. S. An approach to the synthesis of life. *Artificial Life II, Santa Fe Institute Studies in the Sciences of Complexity* (eds Farmer, D. J., Langton, C., Rasmussen, S. & Taylor, C.) **Vol. 11 371–408 (Addison Wesley,** Redwood City, California, 1991).
19. Ray, T. S. Tierra v. 5.0, with documentation. Available via anonymous ftp from the Tierra home page at http://www.isd.atr.co.jp/~ray/tierra
20. Wilke, C. O., Wang, J. L., Ofria, C., Lenski, R. E. & Adami, C. Evolution of digital organisms at high mutation rates leads to survival of the flattest. *Nature* **412,** 331–333 (2001).
21. Yedid, G. & Bell, G. Microevolution in an electronic microcosm. *Am. Nat.* **157,** 465–487 (2001).
22. Mani, G. S. & Clarke, B. C. Mutational order: a major stochastic process in evolution. *Proc. R. Soc. Lond. B* **240,** 29–37 (1990).
23. Johnson, P. A., Lenski, R. E. & Hoppensteadt, F. C. Theoretical analysis of divergence in mean fitness between genetically identical populations. *Proc. R. Soc. Lond. B* **259,** 125–130 (1995).
24. Wahl, L. M. & Krakauer, D. C. Models of experimental evolution: the role of genetic chance and selective necessity. *Genetics* **156,** 1437–1448 (2000).
25. Adami, C. Learning and complexity in genetic auto-adaptive systems. *Physica D* **80,** 154–170 (1995).
26. Adami, C., Ofria, C. & Collier, T. C. Evolution of biological complexity. *Proc. Natl Acad. Sci. USA* **97,** 4463–4468 (2000).
27. Spiegelman, S. An approach to the experimental analysis of precellular evolution. *Q. Rev. Biophys.* **4,** 213–253 (1971).

Acknowledgements This research was supported by a Research Grant from the Natural Sciences and Engineering Research Council of Canada to G.B.

Competing interests statement The authors declare that they have no competing financial interests.

Correspondence and requests for materials should be addressed to G.B. (e-mail: graham.bell@mcgill.ca).

Long-term dendritic spine stability in the adult cortex

Jaime Grutzendler, Narayanan Kasthuri & Wen-Biao Gan

Molecular Neurobiology Program, Skirball Institute, Department of Physiology and Neuroscience, New York University School of Medicine, 540 First Avenue, New York, New York 10016, USA

The structural dynamics of synapses probably has a crucial role in the development and plasticity of the nervous system. In the mammalian brain, the vast majority of excitatory axo-dendritic synapses occur on dendritic specializations called 'spines'. However, little is known about their long-term changes in the intact developing or adult animal. To address this question we developed a transcranial two-photon imaging technique to follow identified spines of layer-5 pyramidal neurons in the primary visual cortex of living transgenic mice expressing yellow fluorescent protein. Here we show that filopodia-like dendritic protrusions, extending and retracting over hours, are abundant in young animals but virtually absent from the adult. In young mice, within the 'critical period' for visual cortex development, ~73% of spines remain stable over a one-month interval; most changes are associated with spine elimination. In contrast, in adult mice, the overwhelming majority of spines (~96%) remain

stable over the same interval with a half-life greater than 13 months. These results indicate that spines, initially plastic during development, become remarkably stable in the adult, providing a potential structural basis for long-term information storage.

Changes in synaptic connections occur in various neurological processes ranging from the development of neuronal circuitry, learning and memory, to injury-related recovery[1–6]. In the mammalian nervous system, synaptic connections are rapidly formed and eliminated in early postnatal life, resulting in a functionally wired mature brain[1–3,7,8]. Classic studies have demonstrated time windows of heightened functional and anatomical plasticity, called 'critical periods', during which the developing nervous system can be rapidly and permanently modified by experience[1,9]. In the visual cortex, for example, brief monocular deprivation during a critical period in development, but not in the adult animal, causes lifelong changes in synaptic connections[1,9,10]. The structural basis underlying this transition from a plastic to a more stable adult nervous system is poorly understood. In adulthood, although the nervous system retains a certain capacity to reorganize after peripheral and central alterations of inputs[4–6,11–13], the degree of structural plasticity in the intact adult brain remains largely unknown.

To study the dynamic nature of synaptic structures in the intact central nervous system, we developed a technique that allows long-term imaging of individual dendritic spines in the living mouse by two-photon microscopy (Fig. 1a, b; see also Methods). We used transgenic mice expressing yellow fluorescent protein (YFP) in pyramidal neurons, predominantly in layer 5 of the cortex[14]. As shown in Fig. 1, individual spines and filopodia on branches of apical dendrites in the visual cortex were imaged at high optical resolution through a thin-skull window. The presence of a thinned skull did not seem to interfere with our ability to resolve the thinnest dendritic protrusions such as filopodia (see images with and without skull, as well as high-resolution confocal images of fixed brain slices in Supplementary Information). Dendrites were then relocated at subsequent time points by using as landmarks surrounding meningeal blood vessels and low-magnification image stacks of nearby neuronal processes (Fig. 1a, b).

We began by imaging segments of apical dendrites, typically in layers I and II, of the primary visual cortex over periods of hours in 1-month-old mice. In these young animals we observed two distinct populations of dendritic protrusions: filopodium-like structures (long and thin processes without spine heads) and spines (Figs 1c, d and 2; see also Supplementary Information). On the basis of their length and the ratios between length, head and neck diameter (see Methods), we classified protrusions as either filopodia or spines and found that the ratio of filopodia to spines was ~1:8.4 at this age ($n = 1{,}580$ protrusions, 10 animals; Fig. 1e). Although filopodia, like dendritic spines, can form synaptic contacts[15,16], previous studies suggest that they are more dynamic than spines and are actively involved in synaptogenesis[17–20]. Consistent with previous studies[17–20] was our observation that the vast majority of filopodia ($90.5 \pm 8.1\%$, $n = 60$, two animals) extended or retracted rapidly, with some eliminated and others formed *de novo* during the 4-h observation period (Fig. 1c, d and f). In contrast, only 5 of 476 spines (~1.0%) extended or retracted during the same period (Fig. 1f).

To further examine long-term changes in filopodia and spines in young (1-month-old) animals, identified dendritic segments were imaged over intervals ranging from 3 days to 1 month. We found that most pre-existing filopodia ($86.2 \pm 12.0\%$) were eliminated, and many new ones ($109.5 \pm 36.7\%$) were formed within 3 days, indicating a rapid turn-over of filopodia at this age (Fig. 2e). Because the ratio of filopodia to spines decreased significantly within the next 2–4 weeks (Fig. 1e), the filopodia that formed within this period must have been either converted to spines or eliminated. Indeed, time-lapse imaging over the next 2–4 weeks showed that the vast majority of filopodia were eliminated, and only rarely did they seem to convert into spines (<1%; Fig. 2a, b and e). Because the rate of new spine formation is also very low at this age (see below), we conclude that the vast majority of filopodia between the first and second months of postnatal life do not contribute to the creation of new connections.

In contrast to filopodia, spines were much more stable at this young age, with $94.2 \pm 1.5\%$ ($n = 365$, three animals) remaining

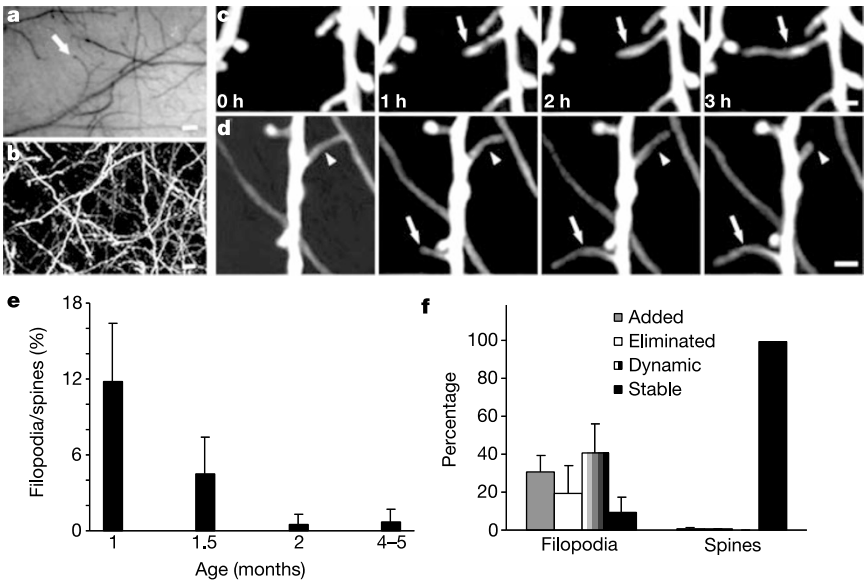

Figure 1 Transcranial two-photon imaging in young animals shows dynamic dendritic filopodia. **a**, Charge-coupled device camera view of the vasculature below the thinned skull. The arrow indicates the region where subsequent two-photon images were obtained. **b**, Two-dimensional projection of a three-dimensional stack of dendritic branches and axons in the primary visual cortex. **c**, **d**, Time-lapse imaging (one hour intervals) in two different 1-month-old animals revealed that filopodia underwent rapid extension (arrows) and retraction (arrowheads), whereas spines on the same dendritic branches remained stable. **e**, Percentage of filopodia (number of filopodia as a percentage of number of spines) decreases as a function of age. **f**, Percentage of filopodia and spines added (number of filopodia or spines added as a percentage of the pre-existing number of filopodia or spines), eliminated and showing either dynamic changes or stability over a period of 4 h. Data are presented as means ± s.d. Scale bars, 50 μm (**a**), 5 μm (**b**) and 1 μm (**c** and **d**).

stable over 3 days. Moreover, 81.6 ± 2.7% ($n = 359$, three animals) remained stable over 2 weeks, and 73.1 ± 2.2% ($n = 361$, three animals) remained stable over a 1-month interval (Fig. 2c, d and f). Interestingly, the percentage of spine elimination (26.9 ± 2.2%) was significantly higher than that of spine formation (3.0 ± 2.9%, $P < 0.0001$; *t*-test) over 1 month, indicating that the net number of spines decreases during this period. This is consistent with previous studies in fixed preparations demonstrating a significant net loss of synapses during the development of monkey and human visual cortex[7,21,22].

Studies on fixed preparations also indicate that synaptic density and the total number of spines remain relatively stable in adulthood[7,8,21–23], suggesting that adult spines are either very stable or are undergoing constant turnover with comparable rates of spine formation and elimination. To determine the degree of spine plasticity in adulthood, we followed dendrites in animals of average age 4.2 ± 0.8 months (14 animals) over intervals ranging from hours to months. Consistent with studies both *in vitro* and in fixed preparations showing a developmental downregulation of rapidly motile filopodia[17–20], we found an almost complete absence of filopodia in adult mice (5 of 630 protrusions, five animals; Fig. 1e and see also Supplementary Information). Furthermore, time-lapse imaging showed that only 2 of 208 dendritic protrusions (two animals) were identified anatomically as filopodia and underwent morphological changes during a 4-h observation period. Neither extension nor retraction was found in 206 spines examined over the same interval. Because filopodia are scarce in adults (<1%), we did not classify dendritic protrusions into filopodia and spines in our subsequent studies of long-term changes in adults.

When imaged over a 3-day interval, we found that in adults, the number and location of spines remained essentially unchanged (99.3 ± 0.7%, $n = 408$, three animals; Fig. 3a–d and m). Remarkably, when the viewing interval was extended to 1 month, 96.5 ± 2.2% of spines were still stably maintained (3.5% eliminated) and the number of new spines was only 3.2 ± 2.1% of the pre-existing ones ($n = 389$, five animals; Fig. 3m). Over a 2-month period, 92.4 ± 1.4% of spines remained stable, and 5.5 ± 2.0% were added ($n = 437$, four animals; Fig. 3e–h and m). In two animals imaged over a 4-month period, 80.4 ± 2.0% of spines remained stable and 9.5 ± 3.8% were added ($n = 101$). Finally, even older animals (10 months old) showed similar rates of spine elimination and formation over a 1-month interval (Fig. 4a). Thus, spines are remarkably stable over long periods in the adult.

Although the number and distribution of adult spines remained largely constant, many spines did undergo marked changes in length or head diameter over 3-day and 1-month periods (Fig. 3i–l). However, we did not observe a trend towards spine enlargement or reduction over either interval ($n = 50$ over 3 days, and $n = 48$ over 1 month; $P > 0.3$; *t*-test). The occurrence of change in the length or diameter of spines was greater during a 1-month interval than over a 3-day interval (*F*-test of variance, $P < 0.000024$ for spine length and $P < 0.0037$ for spine diameter), suggesting that these morphological changes accumulate progressively with time in adult mice and are unlikely to be due to rotational or movement artefacts. Because spine diameter and length are well correlated with the size of the postsynaptic density and the magnitude of signals transmitted to the dendritic shaft[24,25], changes in spine morphology could therefore provide a mechanism of modulating synaptic efficacy.

As shown in Fig. 4a, the rate of spine elimination decreases during post-natal development, whereas the rate of spine formation remains largely unchanged across different ages. On the basis of the observed rates of spine elimination and formation in animals

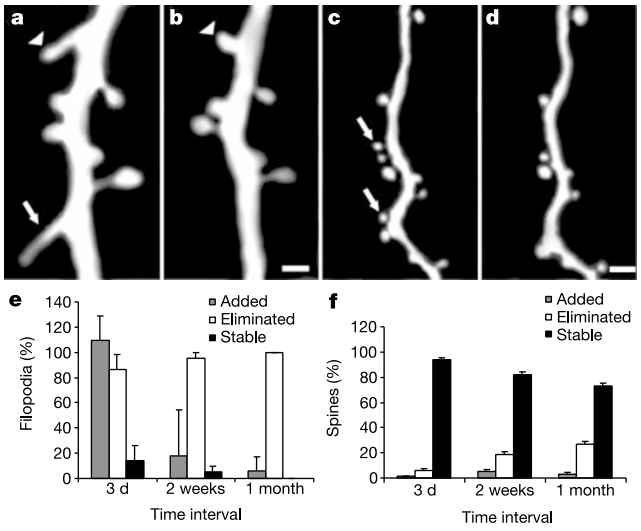

Figure 2 Dendrites in young (1-month-old) animals show predominantly spine and filopodia elimination over long intervals. **a**, **b**, Repeated imaging of dendritic branches over a 1-month interval revealed one filopodium that retracted (arrow) and another that converted into a new spine (arrowheads) by the second view (**b**). **c**, **d**, Repeated imaging of dendritic branches taken 1 month apart revealed the elimination of two spines (arrows) by the second view (**d**). **e**, Percentage of filopodia added (number of filopodia added as a percentage of the pre-existing number of filopodia), eliminated or stable as a function of viewing interval. **f**, Percentage of spines added, eliminated or stable as a function of viewing interval. Data are presented as means ± s.d. Scale bar, 1 μm.

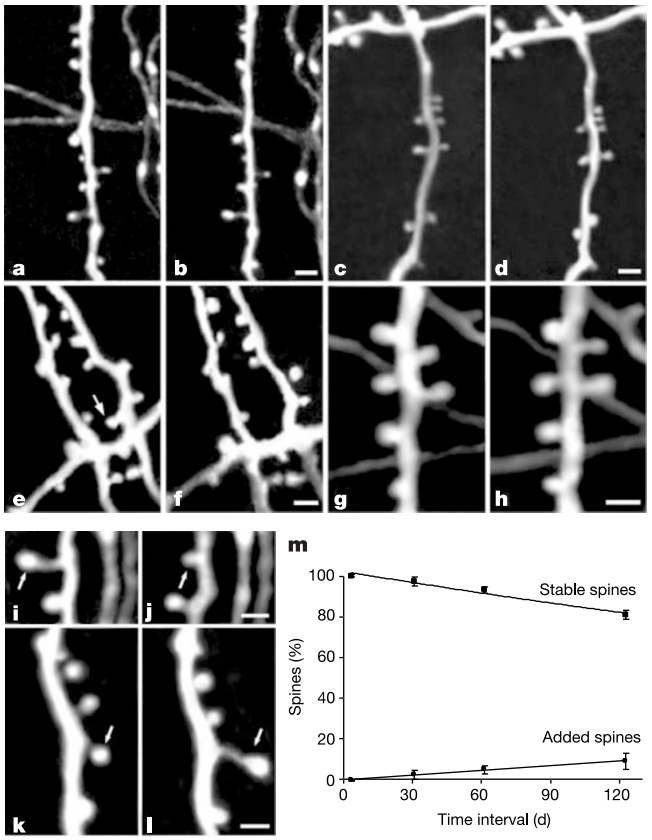

Figure 3 Dendritic spines in adult mice demonstrate long-term stability. **a** and **b**, **c** and **d**, Dendritic branches from two animals imaged 3 d apart show the same spines at the same locations. **e** and **f**, **g** and **h**, Repeated imaging of dendritic branches from two animals (4 months old) imaged 2 months apart show little change in spine number or location. The arrow in **e** points to a spine that is eliminated in the second view (**f**). **i** and **j**, **k** and **l**, Repeated imaging in adult animals shows spine morphology changes over a 1-month interval (see Methods). Spine length and head diameter were reduced markedly (**i**, **j**) or substantially increased by the second view (**k**, **l**). **m**, Percentage of spines that remained stable or were added as a function of imaging interval for adult animals (4.2 ± 0.8 months old, $n = 14$). Data are presented as means ± s.d. Scale bars, 1 μm.

aged 1–6 months, we calculated changes in total spine number as a function of age. These data were well fitted by a single-exponential equation (Fig. 4b; $70.0\% + 30.0\% \times (0.5)^{t/15.63\ \text{days}}$; $\chi^2 = 8.4$), indicating that after the first few months of postnatal development, the total number of spines remains relatively constant in adulthood[7,8,21–23]. For a further quantitative assessment of changes in spine stability in the developing and adult animal, we calculated the average half-lives of spines in animals of different ages. We found that the decline in spine number in animals aged 1–2 months (Fig. 2f) was best fitted by a single-exponential equation ($68.1\% + 31.6\% \times (0.5)^{t/11.3\ \text{days}}$; $\chi^2 = 0.13$), suggesting that ~32% of spines are eliminated with a half-life of 11.3 days while the rest (68%) remain constant. In contrast, assuming that all spines are eliminated at a similar rate, spines in the adult animal (~4 months of age; Fig. 3m) would have an average half life of ~13.2 months ($100.7\% \times (0.5)^{t/396\ \text{days}}$; $\chi^2 = 6.7$). The switch from short to long spine half-life is well correlated with the end of the critical period in the mouse visual cortex[10], indicating that spine stabilization might underlie the transition from a functionally plastic nervous system, during the critical period, to a less malleable one in adulthood.

Because experimental factors such as phototoxicity, anaesthesia, tissue injury, YFP expression and dendritic rotation between views would be more likely to induce artificial changes rather than long-term stability, we would have at most underestimated the degree of long-term spine stability. In addition, our observation of spine stability in mature mice but not in young ones suggests further that it is unlikely that these various factors induced artificial long-term stability selectively in adults. Because we obtained data primarily from spines located in cortical layers I and II, areas that have not traditionally been used to study synaptic plasticity, we do not know whether our observations of spine stability can be generalized to the entire dendritic tree of layer-5 pyramidal cells, different neuronal types, or neurons in regions other than the visual cortex. Further investigation with improved imaging approaches and new mouse models will be necessary to address these questions. However, because the time course of synaptogenesis and synapse elimination have been shown to be similar in various regions of the brain[8,21,23], it is likely that other cortical areas share similar developmental regulation of spine stability. Indeed, preliminary observations over a 2-week interval suggest that spines are also remarkably stable in mature and less so in younger mouse barrel cortex (J.G. and W.-B.G., unpublished observations).

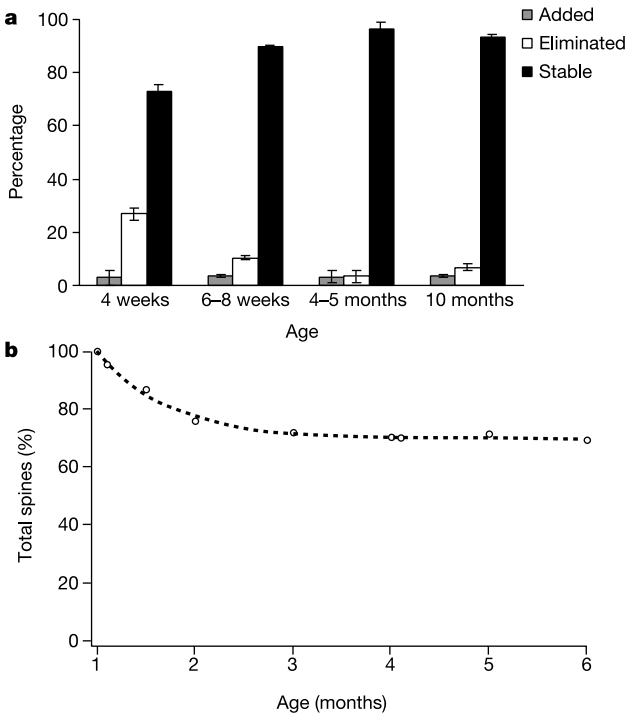

Figure 4 Spine stability increases with age. **a**, Spine stability, formation and elimination over 1-month intervals as a function of age. Data are presented as mean ± s.d. **b**, Percentage of total number of spines as a function of age. The data are fitted by a single-exponential equation (total percentage = $70.0\% + 30.0\% \times (0.5)^{t/15.63\ \text{days}}$, $\chi^2 = 8.4$).

Although adult spines are stable over many months, it is not clear whether axonal terminals are stable or undergo constant turnover. In the peripheral nervous system, long-term *in vivo* imaging has revealed different degrees of synaptic structural stability and dynamism. For example, axon terminals in the young adult autonomic nervous system show gradual changes over periods of weeks and months[26,27]. Yet mouse neuromuscular junctions[28] and submandibular ganglia (W.-B.G., G. Feng, J. R. Sanes and J. W. Lichtman, unpublished observations) maintain axonal branching patterns over many months in adulthood. Thus, as with spines, presynaptic axonal terminals might also demonstrate long-term stability in adulthood.

Our results show that dendritic spines in adult animals, past the critical period for the visual cortex, are remarkably stable with a half-life of more than 13 months (Supplementary Information). The gradual decline of spine plasticity extending into advanced postnatal development indicates that structural plasticity in young adulthood is significantly different from that in the more mature animal[13,26,27]. The long-term stability of spines in the adult brain suggests that synapses can be maintained over the lifetime of an animal and could provide a structural basis for long-term information storage. In addition, the changes in spine length and diameter that we observed could provide a basis for short-term storage of information and could be involved in rapid plasticity, such as lesion-driven and experience-driven cortical remodelling[5,6,11–13]. Such alterations in synaptic efficacy might ultimately regulate the formation and elimination of spines over longer periods and lead to long-term changes in neuronal circuitry. The extent and the timescale over which neuronal activity modulates adult spine stability require future studies. □

Methods

Transgenic mice

Transgenic mice (H–line[14]) were purchased from Jackson Laboratory and were housed and bred in Skirball Institute's animal facilities. All experiments were performed in accordance with animal protocols.

Surgical procedure for *in vivo* imaging

Mice aged 1–10 months were anaesthetized with an intraperitoneal injection (5.0 ml per kg body weight) containing 17 mg ml^{-1} ketamine and 1.7 mg ml^{-1} xylazine in 0.9% NaCl. The skull was exposed with a midline scalp incision and a region (~1 mm in diameter) over primary visual cortex was located based on stereotactic coordinates. A high-speed drill (Fine Science Tools, Foster City, California, USA) was carefully used to reduce the skull thickness by ~50%. To avoid damaging (evidenced by dendritic blebbing, for example) the underlying cortex by friction-induced heat, a cool sterile solution was added to the skull periodically, and drilling was intermittent to permit heat dissipation. Skull thinning was completed by scraping the cranial surface with a micro-surgical blade (Surgistar no. 6400). For optimal image quality, skull thickness was reduced to a very thin layer (~30–50 μm).

To reduce respiration-induced movements, the skull was glued (ethyl cyanoacrylate; Elmer Products no. KG-585) to a stainless steel plate 400 μm thick with a central opening for skull access. The plate was screwed to two lateral bars located on both sides of the mouse head and fixed to a metal base. After imaging, the plate was detached from the skull, the scalp was sutured, and the animal was returned to the cage until the next viewing.

In vivo imaging of dendrites

The animal was inserted under a custom-made two-photon microscope similar to a previously described set-up[29]. The Ti-sapphire laser was tuned to the excitation wavelength for YFP (920 nm) at a low laser power (<40 mW at the sample) to minimize the possibility of phototoxicity. A stack of image planes was acquired by using a water-immersion objective lens (60 ×, 0.9 numerical aperture; Olympus), an external detector and a digital zoom of 3.0–4.0 ×. The imaging depth was ~100–200 μm from the pial surface and the step size was 0.70 μm. Two-dimensional projections of three-dimensional image stacks containing dendritic segments of interest were used for all figures.

Data quantification

The same dendritic segments (~5–20 μm in length; see Figs 2 and 3) were identified from three-dimensional image stacks taken from both views with high image quality (ratio of signal to background noise >4:1). These randomly chosen segments are probably mostly from different parent cells because of the high density of labelled neurons (>33 cells per 6,000 μm^2). The number and location of dendritic protrusions (protrusion length was more than one-third of dendritic shaft diameter) were identified in each view without prior knowledge of the animal's age, the interval between views or the order of the views. The total number of spines (N) was pooled from dendritic segments of different animals. Data throughout the text are presented as means ± s.d.

Filopodia were identified as long thin structures (generally larger than twice the average spine length, ratio of head diameter to neck diameter <1.2:1 and ratio of length to neck diameter >3:1). The remaining protrusions were classified as spines. Three-dimensional stacks were used to ensure that tissue movements and rotation between imaging intervals did not influence spine identification. Spines or filopodia were considered the same between two views on the basis of their spatial relationship to adjacent landmarks and their relative position to immediately adjacent spines (Figs 2 and 3). Spines in the second view were considered different if they were more than 0.7 μm from their expected positions based on the first view.

We chose 0.7 μm as a cut-off distance because apparent spine position can shift by up to ~0.3 μm in either direction along the axis of dendritic shafts owing to changes in spine morphology, slight tissue rotation and movements related to brain pulsation. We estimate the imaging resolution of our two-photon microscope (60 ×, numerical aperture 0.9, at 920 nm) to be ~0.7 μm. We found no significant changes in adult spine stability with three different cut-off distances (0.5, 0.7 and 0.9 μm), showing that our conclusion of spine stability is not dependent on minor changes in these criteria. Even though slight rotations of shafts and protrusions could either obscure existing spines (suggesting spine elimination) or reveal previously hidden spines (suggesting spine addition), such rotational artefacts would only underestimate the amount of stability observed.

For quantification of changes in spine morphology, we minimized the possibility of rotational artefacts by preselecting from three-dimensional image stacks only spines parallel to the imaging plane in both views. Dendrites containing saturated pixels were excluded. Imaging software (NIH ImageJ) was used to measure the spine length and head diameter of identical spines between views. The edges of spines were detected with a Sobel detector algorithm (ImageJ).

Curve fitting was done with the user-defined fitting function on Igor Pro (WaveMetrics, Lake Oswego, Oregon, USA). The single-exponential function was fitted to the data by using the built-in iterative Levenberg–Marquardt function to minimize χ^2.

Received 28 August; accepted 4 November 2002; doi:10.1038/nature01276.

1. Hubel, D. H., Wiesel, T. N. & LeVay, S. Plasticity of ocular dominance columns in monkey striate cortex. *Phil. Trans. R. Soc. Lond. B* **278,** 377–409 (1977).
2. Rakic, P., Bourgeois, J. P. & Goldman-Rakic, P. S. Synaptic development of the cerebral cortex: implications for learning, memory, and mental illness. *Prog. Brain Res.* **102,** 227–243 (1994).
3. Lichtman, J. W. & Colman, H. Synapse elimination and indelible memory. *Neuron* **25,** 269–278 (2000).
4. Buonomano, D. V. & Merzenich, M. M. Cortical plasticity: from synapses to maps. *Annu. Rev. Neurosci.* **21,** 149–186 (1998).
5. Florence, S. L., Taub, H. B. & Kaas, J. H. Large-scale sprouting of cortical connections after peripheral injury in adult macaque monkeys. *Science* **6,** 1117–1121 (1998).
6. Jones, E. G. & Pons, T. P. Thalamic and brainstem contributions to large-scale plasticity of primate somatosensory cortex. *Science* **282,** 1121–1125 (1998).
7. Lund, J. S., Boothe, R. G. & Lund, R. D. Development of neurons in the visual cortex (area 17) of the monkey (*Macaca nemestrina*): a Golgi study from fetal day 127 to postnatal maturity. *J. Comp. Neurol.* **176,** 149–188 (1977).
8. Rakic, P., Bourgeois, J. P., Eckenhoff, M. F., Zecevic, N. & Goldman-Rakic, P. S. Concurrent overproduction of synapses in diverse regions of the primate cerebral cortex. *Science* **11,** 232–235 (1986).
9. Shatz, C. J. & Stryker, M. P. Ocular dominance in layer IV of the cat's visual cortex and the effects of monocular deprivation. *J. Physiol. (Lond.)* **281,** 267–283 (1978).
10. Antonini, A., Fagiolini, M. & Stryker, M. P. Anatomical correlates of functional plasticity in mouse visual cortex. *J. Neurosci.* **1,** 4388–4406 (1999).
11. Bao, S., Chan, V. T. & Merzenich, M. M. Cortical remodelling induced by activity of ventral tegmental dopamine neurons. *Nature* **412,** 79–83 (2001).
12. Kleim, J. A. *et al.* Selective synaptic plasticity within the cerebellar cortex following complex motor skill learning. *Neurobiol. Learn. Mem.* **69,** 274–289 (1998).
13. Knott, G. W., Quairiaux, C., Genoud, C. & Welker, E. Formation of dendritic spines with GABAergic synapses induced by whisker stimulation in adult mice. *Neuron* **34,** 265–273 (2002).
14. Feng, G. *et al.* Imaging neuronal subsets in transgenic mice expressing multiple spectral variants of GFP. *Neuron* **28,** 41–51 (2000).
15. Fiala, J. C., Feinberg, M., Popov, V. & Harris, K. M. Synaptogenesis via dendritic filopodia in developing hippocampal area CA1. *J. Neurosci.* **18,** 8900–8911 (1998).
16. Dunaevsky, A., Blazeski, R., Yuste, R. & Mason, C. Spine motility with synaptic contact. *Nature Neurosci.* **4,** 685–686 (2001).
17. Dailey, M. E. & Smith, S. J. The dynamics of dendritic structure in developing hippocampal slices. *J. Neurosci.* **16,** 2983–2994 (1996).
18. Ziv, N. E. & Smith, S. J. Evidence for a role of dendritic filopodia in synaptogenesis and spine formation. *Neuron* **17,** 91–102 (1996).
19. Dunaevsky, A., Tashiro, A., Majewska, A., Mason, C. & Yuste, R. Developmental regulation of spine motility in the mammalian central nervous system. *Proc. Natl Acad. Sci. USA* **96,** 13438–13443 (1999).
20. Lendvai, B., Stern, E. A., Chen, B. & Svoboda, K. Experience-dependent plasticity of dendritic spines in the developing rat barrel cortex *in vivo*. *Nature* **404,** 876–881 (2000).
21. Boothe, R. G., Greenough, W. T., Lund, J. S. & Wrege, K. A quantitative investigation of spine and dendrite development of neurons in visual cortex (area 17) of *Macaca nemestrina* monkeys. *J. Comp. Neurol.* **186,** 473–489 (1979).
22. Huttenlocher, P. R. & de Courten, C. The development of synapses in striate cortex of man. *Hum. Neurobiol.* **6,** 1–9 (1987).
23. Bourgeois, J. P., Goldman-Rakic, P. S. & Rakic, P. Synaptogenesis in the prefrontal cortex of rhesus monkeys. *Cereb. Cortex* **4,** 78–96 (1994).
24. Harris, K. M. & Stevens, J. K. Dendritic spines of CA 1 pyramidal cells in the rat hippocampus: serial electron microscopy with reference to their biophysical characteristics. *J. Neurosci.* **9,** 2982–2997 (1989).
25. Murthy, V. N., Schikorski, T., Stevens, C. F. & Zhu, Y. Inactivity produces increases in neurotransmitter release and synapse size. *Neuron* **32,** 673–682 (2001).
26. Purves, D. & Hadley, R. D. Changes in the dendritic branching of adult mammalian neurones revealed by repeated imaging *in situ*. *Nature* **315,** 404–406 (1985).
27. Purves, D., Voyvodic, J. T., Magrassi, L. & Yawo, H. Nerve terminal remodeling visualized in living mice by repeated examination of the same neuron. *Science* **238,** 1122–1126 (1987).
28. Lichtman, J. W., Magrassi, L. & Purves, D. Visualization of neuromuscular junctions over periods of several months in living mice. *J. Neurosci.* **7,** 1215–1222 (1987).
29. Majewska, A., Yiu, G. & Yuste, R. A custom-made two-photon microscope and deconvolution system. *Pflügers Arch. Eur. J. Physiol.* **441,** 398–408 (2000).

Supplementary Information accompanies the paper on *Nature*'s website (http://www.nature.com/nature).

Acknowledgements We thank J. Lichtman, S. Burden and R. Yuste for critical comments on this manuscript. This work was supported by grants from the National Institutes of Health and the Ellison Foundation to W.-B.G. and by an Irene Diamond grant to M. L. Dustin for purchasing the imaging system.

Competing interests statement The authors declare that they have no competing financial interests.

Correspondence and requests for materials should be addressed to W.-B.G. (e-mail: gan@saturn.med.nyu.edu).

A role for casein kinase 2α in the *Drosophila* circadian clock

Jui-Ming Lin*†, Valerie L. Kilman*†, Kevin Keegan*, Brie Paddock*, Myai Emery-Le‡, Michael Rosbash‡ & Ravi Allada*§

** Department of Neurobiology and Physiology, and § Department of Pathology, Northwestern University, Evanston, Illinois 60208, USA*
‡ Howard Hughes Medical Institute, Brandeis University, Waltham, Massachusetts 02454, USA
† These authors contributed equally to this work

Circadian clocks drive rhythmic behaviour in animals and are regulated by transcriptional feedback loops[1,2]. For example, the *Drosophila* proteins Clock (Clk) and Cycle (Cyc) activate transcription of *period* (*per*) and *timeless* (*tim*). Per and Tim then associate, translocate to the nucleus, and repress the activity of Clk and Cyc. However, post-translational modifications are also critical to proper timing. Per and Tim undergo rhythmic changes in phosphorylation[1], and evidence supports roles for two kinases in this process: Doubletime (Dbt) phosphorylates Per[3,4], whereas Shaggy (Sgg) phosphorylates Tim[5]. Yet Sgg and Dbt often require a phosphoserine in their target site[6,7], and analysis of Per phosphorylation in *dbt* mutants[3,8] suggests a role for other kinases. Here we show that the catalytic subunit of *Drosophila* casein kinase 2 (CK2α) is expressed predominantly in the cytoplasm of key circadian pacemaker neurons. *CK2α* mutant flies show lengthened circadian period, decreased CK2 activity, and delayed nuclear entry of Per. These effects are probably direct, as CK2α specifically phosphorylates Per *in vitro*. We propose that CK2 is an evolutionary link between the divergent circadian systems of animals, plants and fungi.

To identify new components of circadian clocks, we screened